Comparing numerical modelling finite element results with full scale instrumented pile response in weakly to moderately cemented soil

B. S. Riyat[1], MIEAust CPEng, S. W. Lee[2], FICE (UK), and S. Y. Fok[3]

[1]Senior Associate Geotechnical Engineer, WSP Golder, Building 7, Botanica corporate park, 57/588 Swan ST, Richmond VIC 3121; PH (+61) 3 8862 3684; email: bhavik.riyat@wsp.com
[2]Former Principal, WSP Golder, 7th Floor, One Kowloon, 1 Wang Yuen Road, Kowloon Bay, Hong Kong, PH (+852) 6036 3679; email: geoswlee@gmail.com
[3]Assistant Engineer, WSP Golder, 7th Floor, One Kowloon, 1 Wang Yuen Road, Kowloon Bay, Hong Kong, PH (+852) 66761060; email: sunny.fok@wsp.com

ABSTRACT

Design of drilled and grouted piles in cemented soils remains one of the challenging geotechnical problems mainly due to the variable degree of cementation in the carbonate soil and poses uncertainties to the design of foundations for offshore wind farms structures. Carbonate soils encountered in offshore Australia have embedded layers of loose and compressible cemented soft rocks to well-cemented calcarenites. The purpose of this paper is to undertake finite element analyses using PLAXIS software to quantify pile-soil interaction and predict pile response and load distribution along the pile length under various loading conditions. The results from full scale instrumented piles in weak to moderately cemented soils are presented to draw the comparison between experimental and numerical results. The results from in situ (cone penetration test, CPT) and advanced laboratory testing (constant normal stiffness, CNS) on variable cemented soils that replicate the loading imposed by waves on offshore wind farm structure are used to demonstrate strength degradation in carbonate materials during cyclic loading.

Keywords: Numerical analysis, full scale instrumented pile, PLAXIS, pile-soil interaction

1 INTRODUCTION

Typical structures like offshore wind farms, high-rise buildings and cut and cover metro stations require an adequate foundation system to satisfy ultimate and serviceability limit conditions against uplift forces. In the offshore wind structure conditions, environmental (i.e., wave, currents and wind) and loads produced due to vibration caused by the blade shadowing effect (referred as 2P/3P). In onshore structures, mainly high ground water pressure acting on the base slab of cut and cover structure contribute to uplift forces.

Mainly two components, one weight of the super structure and second is the shaft friction acting along the pile length resist the uplift force. It is important to use more established reliable correlation to estimate shaft capacity of piles, since the shaft capacity depends on the installation type of pile and stratigraphy. In offshore environment, calcareous soils varying from soft uncemented silts to dense well cemented calcarenite and limestone, as encountered in the North West Shelf of Western Australia, pose significant challenges in design. These challenges are further exacerbated by the cost and difficultly of performing full scale load tests in offshore. Drilled and grouted piles are preferred over driven piles in calcareous sediments due to the well documented low shaft frictions that develop on driven piles. However, Joer and Randolph (1994) show that the shaft friction on drilled and grouted piles exhibits significant post-peak strain softening and degrades rapidly with cycling. This is due to a loss of cementation/bonding with the application of shear strains coupled by contractant response of the materials under cyclic loads that leads to reduction of radial stresses on the pile shaft and consequent loss of shaft friction capacity.

The traditional approach for estimating the shaft friction capacity of drilled and grouted piles in moderately cemented calcareous soils is to use empirical correlations that relate shaft friction with the unconfined compressive strength (UCS) e.g. Abbs and Needham (1985). However, sampling of weak rocks for UCS testing is problematic (and often unfeasible) and recent investigations using instrumented piles have improved the understanding of the factors governing the shaft capacity of drilled and grouted piles in weak rock. Therefore, there is a preference for direct correlations with the Cone Penetration Tests (CPT) end resistance (q_c) e.g., Randolph et al. (1996), Lehane (2011) and Riyat and Lehane (2018).

This paper presents the results obtained from onshore in-situ, full-scale tests carried out in 2010 on instrumented drilled and grouted piles at a calcareous sandstone site at Pinjar, Western Australia. The results are compared with the predicted pile response from a series of two dimensional (2D), axisymmetric finite element (FE) parametric analyses using PLAXIS. The weak rock was modelled using a non-linear elasto-plastic constitutive model, Hardening Soil (HS) (Schanz et al., 1999).

2 SITE SOIL/WEAK ROCK CHARATERIZATION

2.1 In situ testing

The site selected for pile load testing is a limestone quarry in Pinjar located about 25 km north of Perth, Western Australia. The weak rock is described as “medium grade limestone” which is a part of the Tamala Limestone formation. Visual inspection on site from test pits indicates the presence of cemented

bands interlayered with weakly and very weakly cemented material (Guo and Lehane 2016). The carbonate contents measured on the cored samples by Lehane (2011) ranged between 40% and 55% and by Guo and Lehane (2016) were typically 40%±25%, indicating sediment deposits classified as calcareous sandstone according to Clark and Walker (1997). The sample core recovery was poor and ranged between 50% and 75%. Core samples recovered during the site investigation are shown in Figure 1, which indicate deposits comprising cobbles, thin cemented layers of sand matrix with varying cementation from uncemented to weakly cemented.

Figure 1. Photo of typical core recovered

The point load Index (Is50) values for the weakly cemented sample documented in Lehane (2011) were typically 0.15±0.05 MPa and were consistent with the range of Is50 values obtained by Guo and Lehane (2016) on samples recovered from the same site.

A total of eight CPTs were carried out across the site, including three tests in the vicinity of each pile location. The CPT profile presented in Figure 2 shows the spatial variability in end cone resistance (q_c) measured across the site with cemented layers existing at varying depths. Typical q_c values range from 15 MPa to 50 MPa with a few lenses showing q_c in excess of 80 MPa and less than 10 MPa. Few CPTs were terminated at shallow depths of less than 3 m. The variation in the q_c values attributes to the range of cementation with larger q_c values are attributed to high levels of cementation, while lenses with q_c values less than 10 MPa are largely uncemented. Friction ratios (F_r) generally lie between 0.2% and 1.0%, but are occasionally higher in the silty layers, for which q_c values are less than 2 MPa.

In typical offshore conditions, carbonate soils comprise greater than 90% CaCo3 and exhibit much softer response of q_c with thin layers of cementation compared to the onshore response of q_c shown in Figure 2.

Figure 3 shows CPT correlations to determine the soil behaviour type (Robertson, 1990). The majority of the pairs of normalised cone resistance (Q_t) and Friction ratio (F_r) fall within zone 6 and zone 7, indicating sediments comprising clean sands to silty sands and gravely sand to sand, respectively. The results also represent the drained penetration, and increase in cementation is evident in the soil behaviour type plot.

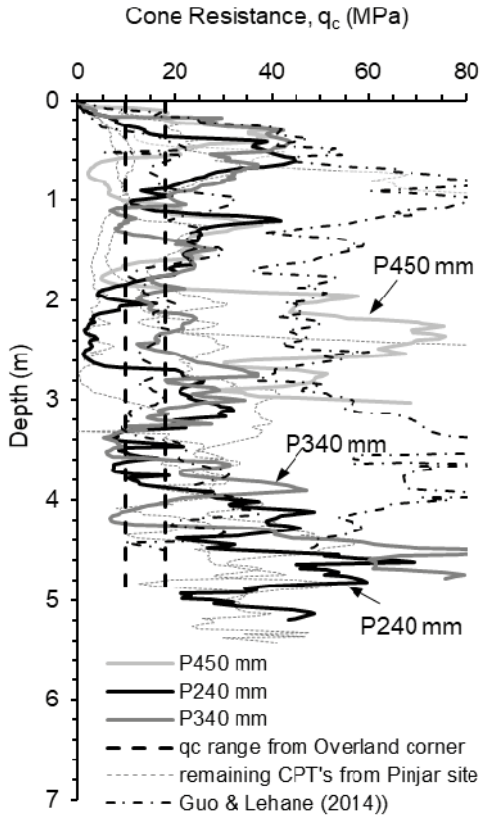

Figure 2. q_c profile of CPT tests from Pinjar site

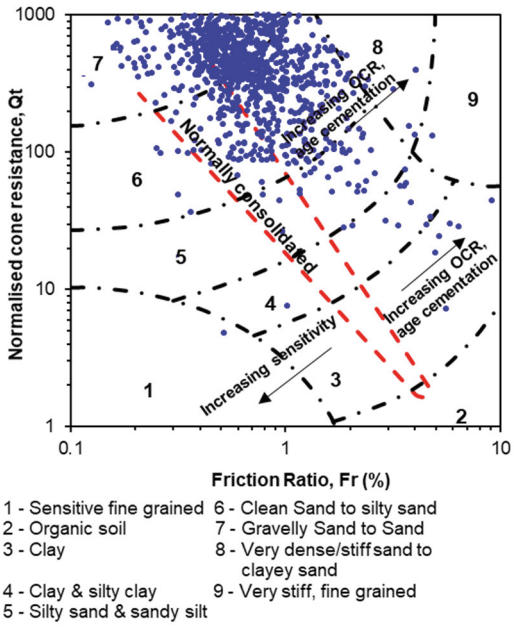

Figure 3. Soil behaviour type classification chart.

2.2 Advanced laboratory testing

Constant normal stiffness (CNS) direct shear tests that replicate the constraint of the surrounding formation around pile surface were carried out to assess the monotonic and cyclic shear response of soil for the design of axially loaded piles, particularly drilled and grouted piles (Johnston et al. 1987). The dilative or contractant response that occurs at the pile

soil interface has a significant effect on the confining stress and hence on peak shaft capacity. In the CNS direct shear test, the vertical load is adjusted to maintain normal stiffness ($K_n = \Delta\sigma_v/\Delta h$) during shearing. The stiffness K_n represents the cavity expansion stiffness of the surrounding rock mass, therefore $K_n = 4G/d_{pile}$, where G is the shear modulus of the weak rock and d_{pile} the pile diameter.

The stress paths from the CNS tests on samples recovered from the site are presented in Figure 4. The samples were first consolidated to a vertical effective stress of 50 kPa before brought to failure through monotonic shearing, maintaining constant stiffness of 400 kPa/mm followed by cyclic loading. The samples indicated a stiff initial response reflection of cementation, with a gradual increase in strength until the shear stress reached the peak. Strain softening response was observed in most of the samples. Higher strength of the sample at depth 2.75 m is possibly due to the dilative response during shearing. From the stress path plot, peak friction angle (φ') varies between 39° and 44°. The findings of the cyclic loading on the CNS test samples are well documented in Lehane (2011) and Riyat and Lehane (2018). In general, large strength reductions were experienced in the initial cycles and the rate of strength degradation reduced with increasing cycles.

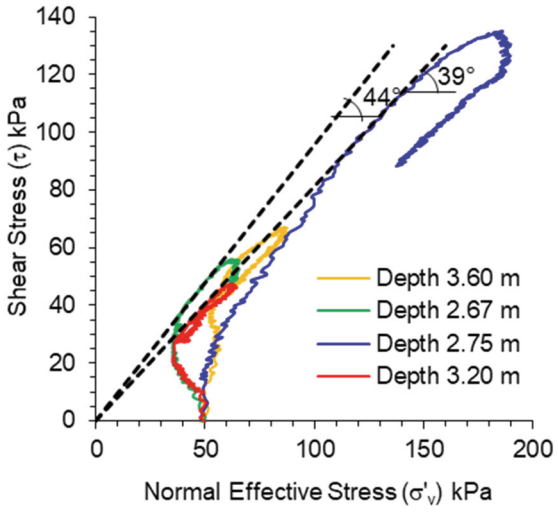

Figure 4. Stress path of monotonic CNS test results

The overall response of strength reduction is well captured in the CNS cyclic test, which is partially due to the shearing nature of the frictional materials but mainly unloading of normal stress with cycles. The volume loss of the sample which can be caused by loss of material (predominant in cemented samples) during cyclic shearing or by sample contraction significantly influences the normal stress. However, loss material was not investigated at the time of testing the samples. The sensitivity of the normal stress on a pile to change in volume in the adjacent soil is captured in DeJong et al. (2003). Randolph et al. (1998) also noted a large reduction in friction under displacement limited to 2-way cyclic loading.

3 FULL SCALE INSTRUMENTED PILE TEST

5 m deep bores for the test piles were drilled in September 2009 using 225 mm, 325 mm and 440 mm diameter augers. Experience with drilling using these augers in similar ground conditions indicated that the final bore diameters formed were 240 mm, 340 mm and 450mm. The holes were tremie grouted with 30 MPa (28-day cube strength) grout before insertion of the steel tubes. These tubes were beaded to ensure good shear transfer and instrumented with 20 quarter bridge strain gauges with two gauges at 10 levels. Tension tests on the piles were performed about 1 month after installation using the test setup described in Lehane (2011). Cyclic testing followed monotonic loading to failure.

3.1 Pile test results

The axial forces for 240 mm pile diameter derived from the axial strains that developed along the pile length for each increment of load applied at the pile head are shown in Figure 8. The unit shaft friction was estimated by taking the difference in axial forces at two subsequent strain gauge levels and divided by the pile surface area. The peak unit shaft friction from the strain gauges data is mobilised between 1.5 m and 3.0 m depth. The β value, which is the ratio of average CPT q_c to the peak shear stress, is typically 90±10 for the 240 mm and 340 mm piles (Lehane, 2011). The 450 mm pile shows a higher β value compared to the smaller diameter piles. The trend is consistent with the results shown by Rollins et al. (2005) for bored piles in sand and by Lehane et al. (2005), where centrifuge results showed the reduction in effective normal stress (smaller dilation) with increased diameter and stress at deeper depths which leads to a corresponding increase in the β values. This also explains the reasoning of micro-piles exhibiting higher shaft friction that corresponds to a lower β .

The load-displacement and cyclic responses observed at the pile heads are well captured and presented in Riyat and Lehane (2018). The peak tensile loads of 1280 kN, 1530 kN and 950 kN were observed for the 240 mm, 340 mm and 450 mm diameter piles, respectively. The significantly lower capacity indicated by the 450 mm pile highlights the variability in the ground conditions at the test site. The 450 mm pile also shows the highest level of post-peak brittleness, indicating ground conditions at this location differed from those at the other two locations which give quite similar peak and ultimate shaft shear stresses.

Comparing the cyclic response of the 240 mm and 340 mm piles, it is observed that higher amplitudes of cyclic load lead to larger cyclic displacement accumulations (Riyat and Lehane, 2018). However, more rapid accumulation of cyclic displacement is observed for the 450 mm pile with similar cyclic load amplitude compared to the 240 mm pile, illustrating the difference in ground conditions at the two respective locations and possibly also reflecting scale effects. The post-cyclic monotonic capacities for the 240 mm, 340 mm and 450 mm piles are 86%, 78% and 60% respectively of the tension capacity.

4 FINITE ELEMENT ANALYSIS

4.1 Tension pile in 2D axisymmetric analysis

PLAXIS 2D axisymmetric model is used to simulate the tension pile load test, as shown in Figure 5. Weakly cemented rock and pile-soil interface are represented by the HS model with parameters provided in Table 1. The Interface elements are used to model a thin zone of intense shearing along the pile shaft between the concrete and the surrounding soil. The interface element can model slipping and gapping/overlapping behaviours, i.e., relative displacement parallel and perpendicular to the interface, respectively. The concrete pile is modelled using volume elements with a linear elastic material representing the concrete properties. The tension load is applied in increments (to simulate pile load tests) as a uniformly distributed load on the pile head. The pile-soil interface is configured by assigning a weakly cemented material with manually reduced strength and stiffness based on an interface factor of 0.67. The interface is extended beyond the pile toe to avoid stress oscillation at pile corners.

The HS model is preferred over the Mohr-Coulomb model as dilatancy cut-off is available in HS model by specifying a maximum void ratio (e_{max}). The input e_{max} is the void ratio at critical state. When e_{max} is reached, the dilation angle is set to zero (PLAXIS, 2021). A halved Young's modulus of 15 GPa is adopted for the concrete to account for reduction in stiffness due to cracks under tension loading. This would overpredict pile displacement under small load increments, but would better predict pile displacement under higher load increments.

4.2 Calibration of soil parameters

The dependency of pile axial response on the soil strength and stiffness properties, such as Young's modulus, friction angle, cohesion, dilatancy angle of the weak rock was investigated by undertaking a large number of parametric analyses. The parametric results are calibrated with the monotonic load-displacement responses of the 240 mm and 340 mm test piles. The 450 mm pile is not used in the calibration due to the difference in ground conditions from the two other piles.

Table 1: Optimal range of HS model parameters

Parameters	Weak rock	Pile-soil interface
γ_{unsat} (kN/m^3)	16	16
γ_{sat} (kN/m^3)	16	16
E_{50}^{ref} (MPa)	180 - 210	95 - 115
E_{oed}^{ref} (MPa)	180 - 210	95 - 115
E_{ur}^{ref} (MPa)	540 - 630	290 - 345
c_{ref} (kPa)	90 - 100	60 - 67
ϕ (°)	42 - 44	31 - 33
ψ (°)	16 - 22	16 - 22
e_0	0.5	0.5
e_{max}	0.53 - 0.56	0.53 - 0.56

The optimal ranges of weak rock and the pile-soil interface properties obtained in the parametric analyses are shown in Table 1. The dilatancy cut-off limited by e_{max} was found to have a significant influence on the predicted tension capacity of the pile, as shown in Figure 6. In the final analyses, an e_{max} of 0.55 was adopted.

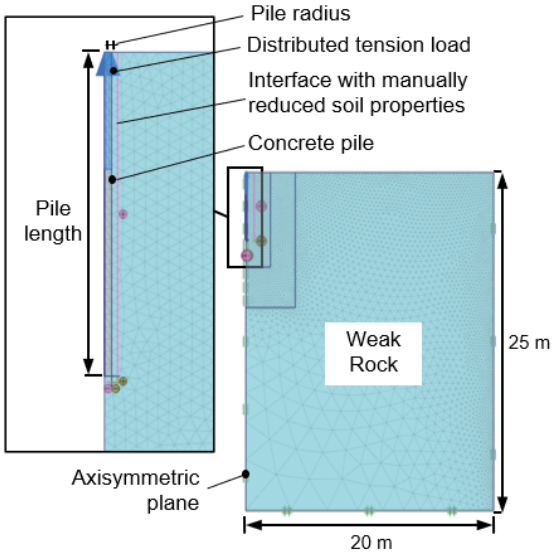

Figure 5. Tension pile load test in PLAXIS 2D

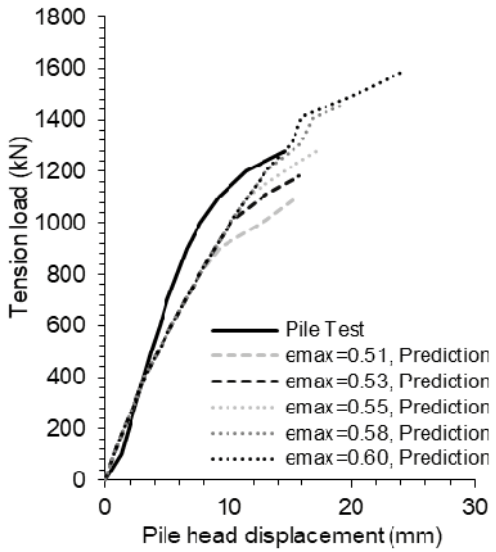

Figure 6. Parametric study of 240mm pile on maximum void ratio

5 COMPARISON BETWEEN NUMERICAL AND FIELD TEST RESULTS

5.1 Shear stress-displacement

Figure 7 compares the average shaft shear stress (τ_{avg}) versus normalised pile head displacement (w/D) between the test piles and the predictions for the 240 mm, 340 mm and 450 mm piles. The predictions for the 240 mm and 340 mm piles are in a reasonable agreement with the field test results, despite generally predicting a softer response. The predicted maximum τ_{avg} for the 450 mm pile

(300 kPa) is about twice the measured value at failure (130 kPa), and this is likely attributed to the presence of weaker material with no cementation in the field.

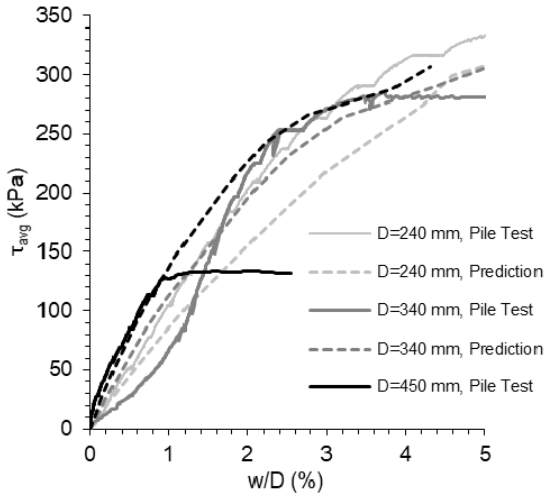

Figure 7. Comparison of τ_{avg} between measurements and predictions

5.2 Axial load, axial strain and shear stress distribution

Figure 8 compares the axial tensile load, axial strain and unit shaft friction for the 240 mm pile between the measurements and predictions. In Figure 8(a), the predicted axial load distribution is comparable with the measured distribution at smaller loads. When the tensile load at pile head is greater than 700 kN, the analysis underpredicts the load distribution between 1m and 2m depth. The results match well at the depths below 2m.

In Figure 8(b), the rate of growth in axial strain is more evident at higher loads in the measured test pile data. This is possibly due to the cracking of concrete occurring at higher loads in the field. The predictions show a relatively constant rate of growth in axial strain due to the adoption of a linear elastic material for concrete. The axial strains are overpredicted at smaller loads and better predicted at higher loads because a halved concrete modulus of 15 GPa was used throughout all load increments.

In Figure 8(c), the predicted trend of distribution of unit shaft friction is generally similar to that measured, despite underpredicting the maximum unit shaft friction values. This could be caused by the simplified ground profile modelled in the analysis, which does not capture the spatial variation of q_c observed in the field that would influence the shaft mobilization.

6 COMPARISON OF PEAK FRICTION BETWEEN NUMERICAL, CASE HISTORY AND FIELD TEST RESULTS

The peak shear stresses (τ_p) predicted from the numerical model are normalised with q_c and plotted against the q_c normalized by atmospheric pressure (p_a) as presented in Figure 9. The measured τ_p/q_c ratios from the test piles at Pinjar and their best-fit mean trend line, the suggested design lower-bound line by Riyat and Lehane (2018), and the field measurements by Joer and Randolph (1994) on grouted driven piles are also presented for comparison.

The predicted τ_p/q_c ratios are in good agreement with the best-fit mean trend line of the three test piles. Comparing to other case histories, the prediction also captures the trend of decreasing τ_p/q_c with increasing q_c/p_a.

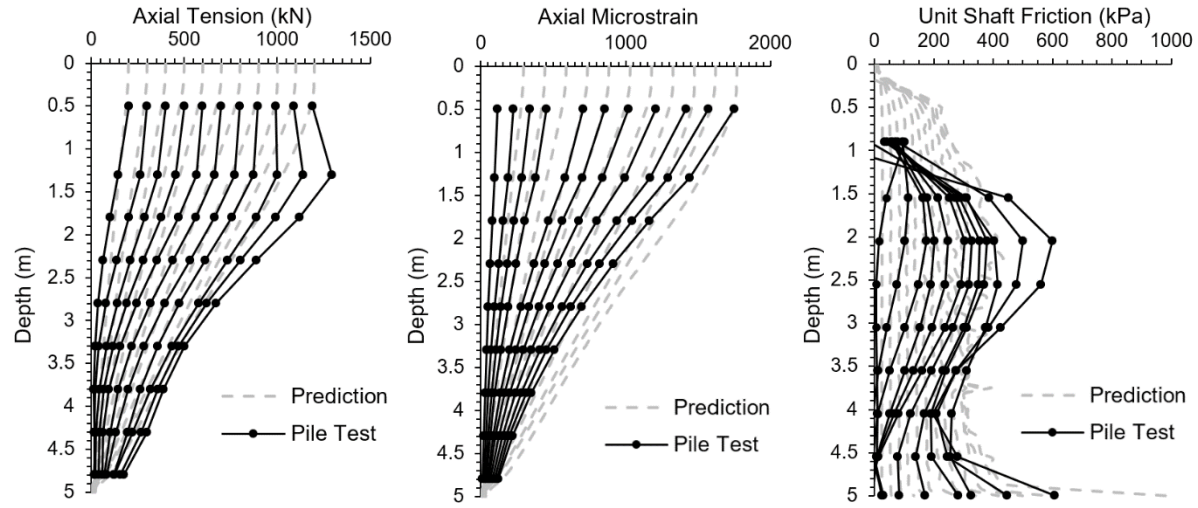

Figure 8. Comparison of axial load (a), axial strain (b) and unit shaft friction (c) in 240mm pile

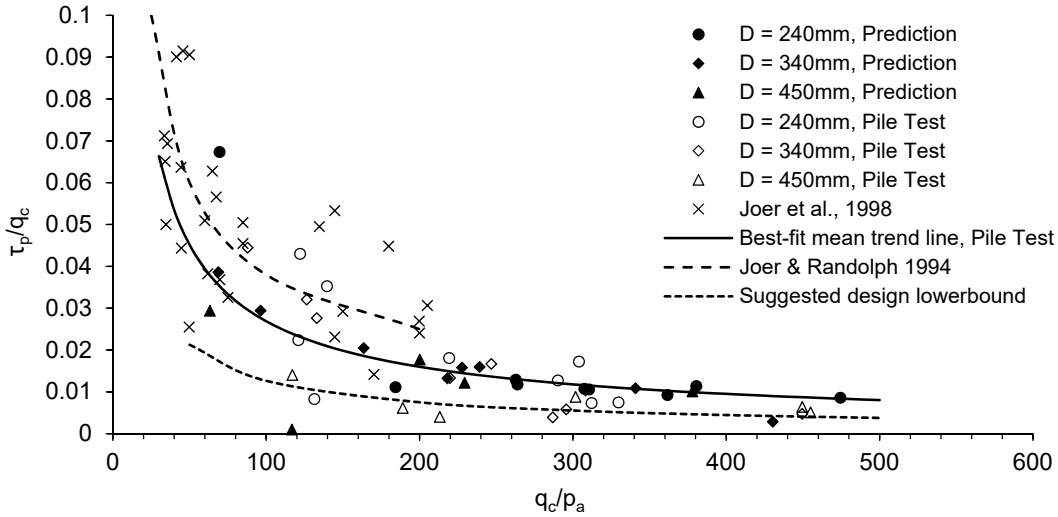

Figure 9. Comparison of τ_p/q_c ratios between test piles, numerical predictions, and case history results

7 CONCLUSION

This paper shows that the CPT results revealed a spatial variation of cone resistance q_c in the weak rock formation and the poor recovery of core samples poses the challenges in obtaining undisturbed samples for strength testing. Thus, making the dependency of design on shaft friction and CPT q_c more favourable.

This paper also presents FE 2D axisymmetric analyses in modelling three instrumented tension pile load tests at Pinjar. Parametric analyses were carried out to obtain a reliable range of soil and soil-pile interface input parameters, and calibrated against the results of high-quality soil/rock testing and pile testing. It is revealed that the dilation at the soil-pile interface affecting normal effective stress acting on the pile shaft has a significant influence on the predicted pile tension capacity. The predicted τ_p/q_c vs q_c/p_a ratios are in good agreement with the case histories in similar ground conditions and pile types.

The low pile tension capacity measured at the 450 mm test pile could be caused by a combination of a reduction in dilation with increased pile diameter and the presence of weakly cemented material.

The FE modelling could be further improved by considering the pile installation effect, pile roughness, constant normal stiffness caused by dilation at soil-pile interface, variation in ground profile, etc.

8 ACKNOWLEDGEMENTS

The authors gratefully acknowledge the support provided by the Arup Design and Technical (DTX) research fund, the on-site assistance from Belpile Pty Ltd and WSP Golder for the use of commercial finite element software 2D Plaxis for numerical modelling.

REFERENCES

Abbs, A.F. and Needham, A.D. 1985. “Grouted piles in weak carbonate rock.” Proc. Offshore Technology Conference, Paper No. OTC 4852, Houston, 105-112.

Clark A.R. and Walker, B.F. 1997. “A proposed scheme for the classification and nomenclature for use in the engineering description of Middle Eastern sedimentary rocks.” Géotechnique 27(3) 93-99.

De Jong, J.T., Randoph, M.F. and White D.J. 2003. “Interface load transfer degradation during cyclic loading: a microscopic investigation.” Soils Found., 43(4):81-93.

Guo, F. and B.M. Lehane. 2016. “Lateral response of piles in weak calcareous sandstone.” Canadian Geotechnical Journal, **53**, 1-11.

Joer, H.A., Randolph, M.F. and Gunasena, U. 1998. “Experimental modelling of the shaft capacity of grouted driven piles.” ASTM Geotech. Test. J., 21(3): 159–168.

Joer, H.A., and Randolph, M.F. 1994. “Modelling of the shaft capacity of grouted driven piles in calcareous Sediments.” Proc, Int Conf. Des. Constr. Deep Found., FHWA Orland. 2: 873-887.

Johnston, I.W., Lam, T.S.K and Williams, A.F. 1987. “Constant normal stiffens direct shear test for rock socketed pile design in weak rock.” Géotechnique 37(1), 83-89.

Lehane B.M., Gaudin C. and Schneider J.A. 2005 “Scale effects on tension capacity for rough piles buries in dense sand.” Geotechnique, 55(10), 709-719

Lehane, B.M. 2011. “Shaft capacity of drilled and grouted piles in calcareous sandstone.” 2nd International Symposium Frontiers in Offshore Geotechnics ISFOG, Perth, 519-524.

PLAXIS. 2021. “Materials Model Manual”. Connect Edition V22.00.

Randolph, M.F., Joer, H.A., Khorshid, M.S. and Hyden, A.M. 1996. “Field and laboratory data from pile load tests in calcareous soils.” Proc. Offshore Technology Conference, Paper No. OTC 7992, Huston, 327-336.

Riyat B.S and Lehane B.M. 2018. “Full scale instrumented pile response in moderately cemented calcareous soil.” Engineering in Chalk, ICE publication.

Robertson, P.K. 1990. “Soil classification using the cone penetration test.” Can. Geotech. J., 27(1); 151-158.

Rollins K.M., Clayton R.J., Mikesell R.C. and Blaise B.C. 2005. “Drilled shaft side friction in gravely soils.” Journal of Geotechnical and Geoenvironmental Engineering, ASCE, 131(8), 987-1003.

Schanz, T., Vermeer, P.A., Bonnier, P.G., 1999. "The hardening soil model: formulation and verification." Beyond 2000 in Computational Geotechnics. Balkema, Rotterdam.